Fiber-Based Generator for Wearable Electronics and Mobile Medication

Junwen Zhong,[†,⊥] Yan Zhang,[‡,§,⊥] Qize Zhong,[†,⊥] Qiyi Hu,[†] Bin Hu,[†] Zhong Lin Wang,[‡,∥] and Jun Zhou[†,*]

[†]Wuhan National Laboratory for Optoelectronics and School of Optical and Electronic Information, Huazhong University of Science and Technology, Wuhan, 430074, China, [‡]Beijing Institute of Nanoenergy and Nanosystems, Chinese Academy of Sciences, Beijing, China, [§]Institute of Theoretical Physics and Key Laboratory for Magnetism and Magnetic Materials of MOE, Lanzhou University, Lanzhou 730000, China, and [∥]School of Materials Science and Engineering, Georgia Institute of Technology, Atlanta, Georgia 30332-0245, United States. [⊥]J.-W. Zhong, Y. Zhang, and Q.-Z. Zhong contributed equally to this work.

ABSTRACT Smart garments for monitoring physiological and biomechanical signals of the human body are key sensors for personalized healthcare. However, they typically require bulky battery packs or have to be plugged into an electric plug in order to operate. Thus, a smart shirt that can extract energy from human body motions to run body-worn healthcare sensors is particularly desirable. Here, we demonstrated a metal-free fiber-based generator (FBG) *via* a simple, cost-effective method by using commodity cotton threads, a polytetrafluoroethylene aqueous suspension, and carbon nanotubes as source materials. The FBGs can convert biomechanical motions/vibration energy into electricity utilizing the electrostatic effect with an average output power density of $\sim$0.1 μW/cm^2 and have been identified as an effective building element for a power shirt to trigger a wireless body temperature sensor system. Furthermore, the FBG was demonstrated as a self-powered active sensor to quantitatively detect human motion.

KEYWORDS: electrostatic induction · fiber-based generator · mobile medication system

Smart garments for monitoring physiological and biomechanical signals of the human body are key sensors for personalized healthcare. However, they typically require bulky battery packs or have to be plugged into an electric plug in order to operate. Thus, a smart shirt that can extract energy from human body motions to run body-worn healthcare sensors is particularly desirable. Here, we demonstrated a metal-free fiber-based generator (FBG) *via* a simple, cost-effective method by using commodity cotton threads, a polytetrafluoroethylene aqueous suspension, and carbon nanotubes as source materials. The FBGs can convert biomechanical motions/vibration energy into electricity utilizing the electrostatic effect with an average output power density of $\sim$0.1 μW/cm^2 and have been identified as an effective building element for a power shirt to trigger a wireless body temperature sensor system. Furthermore, the FBG was demonstrated as a self-powered active sensor to quantitatively detect human motion.

Wearable electronics represents a paradigm shift in consumer electronics for applications such as integration with human body and health/wellness monitors, surgical tools, and body sensor networks (BSN).[1−4] The vision of noninvasive, automated personalized healthcare using wearable wireless medical devices is a new and fast-growing multidisciplinary research area.[5] For example, continuous monitoring of human blood pressure in patients with hypertension can significantly increase medication compliance;[6] real-time monitoring of electrocardiograph traces can be very effective at revealing early stages of heart diseases.[7] Although sensing garments (with the commercial name of Smart shirt) for monitoring physiological and biomechanical signals of the human body have already been invented for healthcare[8] and sports training,[9] they typically require bulky battery packs or have to be plugged into an electric plug in order to operate, which may limit the widespread usage of smart garments.[10−13]

Indeed, fueled by the rapid development of micro- and nanotechnologies, lower power consumption and even self-powered systems have profound impacts for biomedical and portable electronics.[14] Biomechanical energy represents a typical, universally available, and feasible source of continuous power for wearable devices. The human body is a surprisingly rich source of energy

* Address correspondence to jun.zhou@mail.hust.edu.cn.

Received for review March 30, 2014 and accepted April 26, 2014.

Published online April 26, 2014
10.1021/nn501732z

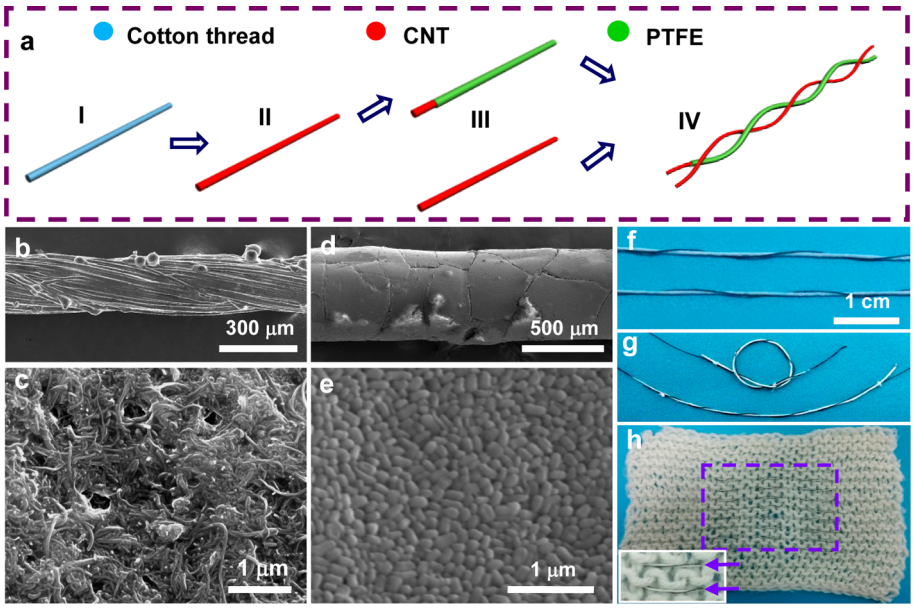

Figure 1. Fabrication of fiber-based generator (FBG). (a) Schematic diagram illustrating the fabricating process of an FBG. SEM images of a carbon nanotube coated cotton thread (CCT) with (b) low and (c) high magnification, respectively. SEM images of polytetrafluoroethylene (PTFE) and carbon nanotube coated cotton thread (PCCT) with (d) low and (e) high magnification, respectively. Digital photography of FBGs (f) with linear shape, (g) with curved shape, and (h) woven into fabric.

including walking, arm swinging, finger motion, and breathing. It is estimated that harvesting even 1−5% of the body's power without significantly increasing the load to the human body would be sufficient to run many body-worn devices.[15] Thus, devices that exploit biomechanical motions as natural sources of energy can be particularly desirable. In the past two decades, researchers have developed multiple routes including electromagnetic fields,[16,17] the piezoelectric effect,[18−27] the electrostatic effect,[28,29] and the triboelectric effect[30−32] toward transforming biomechanical motion into electrical power.

Ideally, if the energy harvesters were implemented as textile-fiber structures, such fibers would provide perfect building elements for a smart shirt, as they could be naturally integrated into fabrics during the weaving process without affecting comfort, flexibility, air permeability, and maneuverability. Qin *et al.* demonstrated a nanogenerator based on the piezoelectric effect using hybrid-structured microfiber-ZnO oxide nanowires,[20] but its structure was very fragile and the power output was so low that this kind of nanogenerator is not feasible to be integrated into textiles for smart garments.[14] Here we introduce a cost-effective, metal-free, fiber-based generator that can convert biomechanical motions/vibration energy into electricity by the electrostatic induction effect. The FBG consists of two entangled modified-cotton threads: one is a carbon nanotube (CNT) coated cotton thread (CCT), and the other is a polytetrafluoroethylene (PTFE) and carbon nanotube coated cotton thread (PCCT). The FBGs can be woven into a commercial textile to form a "power shirt" and used to trigger a wireless body temperature monitor system. Moreover, the FBGs were demonstrated to quantitatively monitor human body motion. This work establishes the first proof-of-concept that the FBG can be woven into fabrics and exploit the biomechanical motions as natural energy sources for wearable electronics and mobile medication applications.

RESULTS AND DISCUSSION

Fabrication of Fiber-Based Generators. The source materials for the FBGs are commodity cotton threads, a PTFE aqueous suspension, and carbon nanotube ink. The detailed fabrication process is schematically shown in Figure 1a and supplementary methods. The cotton threads were first treated by ethanol flame to eliminate redundant fibers (Supplementary Figure S1a and b) and treated by a nitric acid solution to increase the hydrophilicity. The pretreated cotton threads were then coated with multiwalled carbon nanotubes by using a homemade CNT ink *via* a "dipping and drying" method to make them conductive (Figure 1a II).[11] Compared with metal electrodes, CNTs have better adhesion with celluloses due to their mutual strong chemical bonds.[33] Moreover, compared with the thermal evaporation method, which is normally utilized to deposit metal electrodes, "dipping and drying" is a simple and cost-effective method. Scanning electron microscopy (SEM) images shown in Figure 1b and c reveal that the surface of the cotton thread with a diameter of ~240 μm was fully covered by CNTs, with a mass loading density of ~0.207 mg/cm. The final CCTs have a good flexibility and conductivity with a constant resistance of ~0.644 kΩ/cm in both straight and curving condition (Supplementary Figure S2a). The maximum tensile

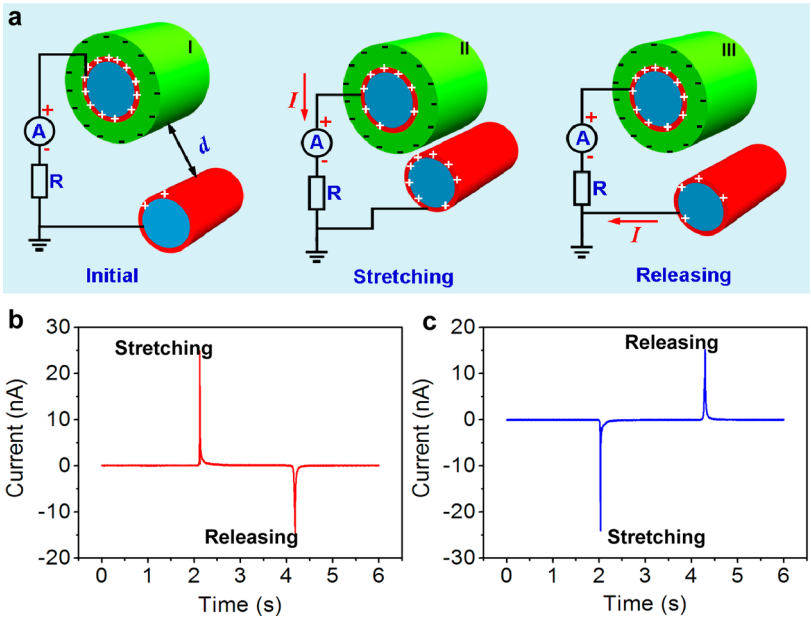

Figure 2. Power generation mechanism of the FBG. (a) Schematic diagram illustrating the power generation mechanism of the FBG with an external load of *R* when the device is at (I) the original, (II) stretching, and (III) releasing states, respectively. The corresponding output current−time curves (d) when forward-connected to the measurement system and (c) when reverse-connected to the measurement system.

stress that can be borne by the CCT and FBG is ~180 and ~210 MPa, respectively (Supplementary Figure S2b).

PCCTs were prepared by coating CCTs with PTFE *via* a "dipping and drying" method (Figure 1a III) followed by a sequence annealing process to enhance the adhesion. As one of the representative electret materials for power generators,[29] PTEF can theoretically retain electrostatic charges on its surfaces for over tens of years.[34] The top view and cross-sectional view SEM images shown in Figure 1d and Figure S1d reveal a core−shell-structured character with a diameter of ~500 μm. There are some minor cracks on the surface of the PCCTs, which may be due to the stress-releasing process. The formation of the cracks can enhance the flexibility of the PCCTs. A high-resolution SEM image shown in Figure 1e indicates that the PTFE layer was composed of oval-like nanoparticles with diameters of less than 200 nm. The PCCTs were polarized *via* oxygen plasma treatment and resulted in net negative electrostatic charges (*Q*) on the PTFE surface, and 40 min of polarization can dramatically increase the surface potential of PCCTs from *ca.* −9 V for fresh samples to *ca.* −660 V (Supplementary Figure S3a). The surface potential decreased to ~470 V in 30 h and could almost maintain this value for more than 20 days. The high stability of the surface potential in PCCTs is beneficial for long-term sustainable applications of the device. Finally, a CCT and a PCCT were entangled with each other to form a lightweight, flexible FBG with double-helix structure (Figure 1a IV, Figure 1f and g). The helix turns and leaving gaps of the FBG can be adjusted, and the two ends of the FBG were fixed by commodity cotton threads. In our study, the FBGs can be easily woven into fabric to form a "power shirt" (Figure 1h).

Proposed Power Generation Mechanism of the Fiber-Based Generators. Although the FBG has a complex "double-helix" structure, the FBG can be approximately regarded as numerous parallel-wire capacitors connected in parallel by ignoring the edge effect. In a simplified model, the equivalent circuit of the FBG with an external load of *R* is illustrated in Figure 2a. In the original state (Figure 2a, I), the PTFE surface, the outer layer of the PCCT, was charged with negative electrostatic charges of *Q* while the CCT was grounded, and the CNT layers in both the PCCT and CCT would produce positive charges of Q_1 and Q_2, respectively, due to the electrostatic induction and conservation of charges, where $Q = -(Q_1 + Q_2)$.[32] Therefore, the charges *Q* on PTFE could be considered as an electric field source.

When the FBG was stretched (Figure 2a, II), a shrinkage of the interfiber gap distance *d* between CCT and PCCT would result in more induced positive charges accumulating in the CNT layer of the CCT because of the electrostatic induction. Accordingly, free electrons of CCT would flow to the CNT layer of PCCT in order to balance the field from *Q*. Thus, this process produces an instantaneous positive current (Figure 2b) (we defined a forward connection for measurement as a configuration with the positive end of the electrometer connected to the CNT electrode of the PCCT). It is necessary to note that the charge *Q* on PTFE will not be annihilated even when it contacts with the CNT-coated fiber, because the electrostatic charges are naturally impregnated into

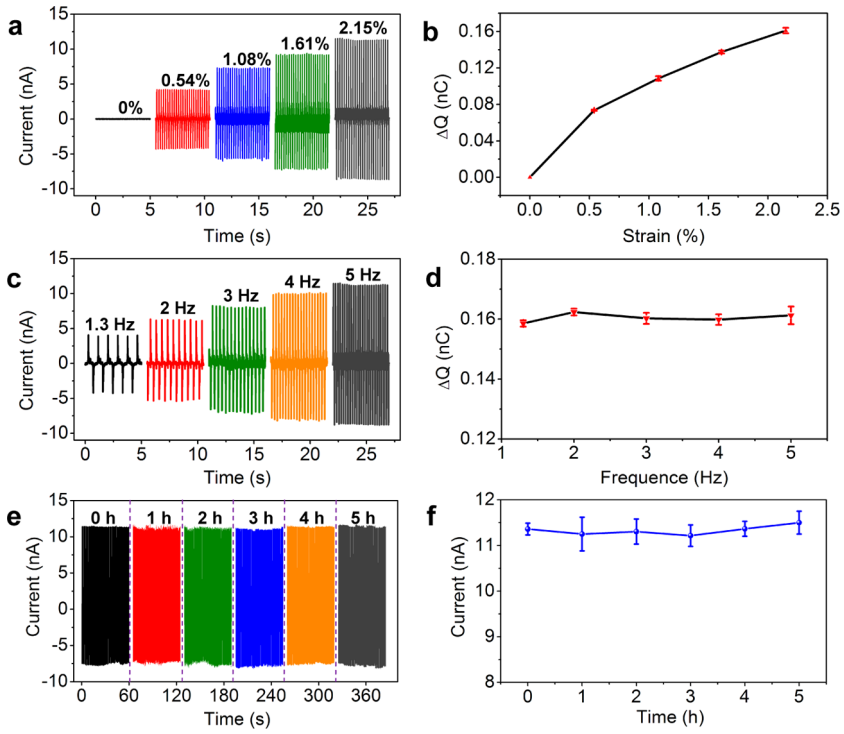

Figure 3. Power generation performance of a single FBG though an external load of 80 MΩ under different testing conditions. (a) Output current−time curve and (b) the corresponding total charge transfer of a FBG varied with stimulation strains of 0, 0.54%, 1.08%, 1.61%, and 2.15% for a given frequency of 5 Hz. (c) Output current−time curve and (d) the corresponding total charge transfer of a FBG varied with stimulate frequencies of 1.3, 2, 3, 4, and 5 Hz for a given strain of 2.15%. (f) Five hours (∼90 000 cycles) continuous power generation of the FBG and (g) the variation of peak output current over time.

the insulator PTFE. In the reverse case, when the FBG was released (Figure 2a III), the device would recover back to its original shape and the internal gap d is increased, resulting in an increase of Q_1 and a decrease of Q_2; thus, an instantaneous negative current could be produced (Figure 2b). Therefore, a stretching−releasing process of the FBG will generate an alternating current (ac) through the load.

As the electrostatic charges remain stable (Supplementary Figure S3b) for a relative long time on the PCCT surface, the FBG can be thought of as a type of variable-capacitance generator. Switching polarity tests were also carried out to confirm that the measured output signals were generated from the FBG rather than from the measurement system (Figure 2c).

Power Generation Performance of a Single Fiber-Based Generator. The typical power generation performance of the FBG with a length of ∼9.0 cm and eight helix turns was systematically studied by periodically stretching and releasing the FBG with controlled frequencies and strains. The measuring system is schematically shown in Figure S4; one end of the FBG was fixed on an *x-y-z* 3D mechanical stage that was mounted tightly on an optical table, while the other end was fixed on a vibration source with controlled frequency. The output current through an external load of 80 MΩ was continuously monitored.

Figure 3a shows the output current of an FBG with an applied strain of 0, 0.54%, 1.08%, 1.61%, and 2.15% at a given frequency of 5 Hz. No current signal was detected when there was no stimulation applied on the FBG. Generally, an increase of strain increased the peak output current, from 3.98 nA at 0.54% to 11.22 nA at 2.15% (Figure S5b). The integration of each current peak can give the total charges transferred between the electrodes, as shown in Figure 3b and Figure S5c, indicating that the total amount of charges transferred increased with the increase of strain, which is consistent with our model discussed above. The output current of an FBG varied with stimulation frequencies of 1.3, 2, 3, 4, and 5 Hz for a given strain of 2.15% is shown in Figure 3c, revealing a clear increasing trend with the increase of frequency. The integrations of each current peak from each of the five different stimulation frequencies are shown in Figure 3d and Figure S5d, indicating that the total amount of the charges transferred almost stays constant at ∼0.16 nC at a given strain of 2.15%. This study indicates that the peak output current is related to both the stimulation frequency and magnitude of strain, while the amount of the transferred charges is related only to the applied strain.

The characterization curve of the dependence of the output power on the external load is shown in Figure S6a. It was measured at a given frequency (5 Hz) and degree of deformation (2.15% strain). The instantaneous output peak power value is 11.08 nW, corresponding to an optimal external load of 100 MΩ.

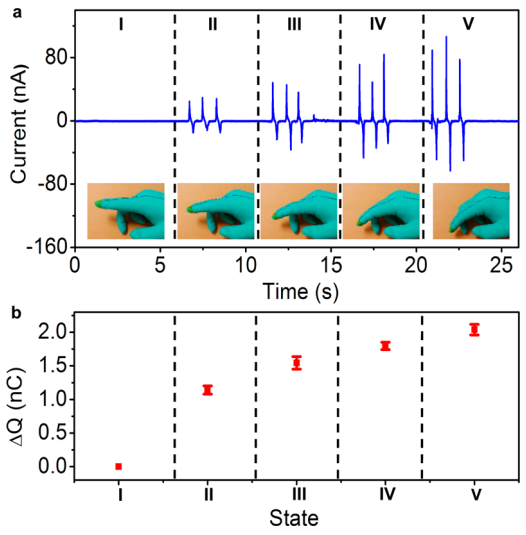

Figure 4. FBG as a self-powered active sensor for body motion detection. (a) Current–time response curve and (b) the corresponding change transfer through an 80 MΩ external load of the FBG that was fixed on an index finger at five different bending–releasing finger motion amplitudes. The down insets in (a) labeled as I, II, III, IV, and V demonstrate the five finger-motion states.

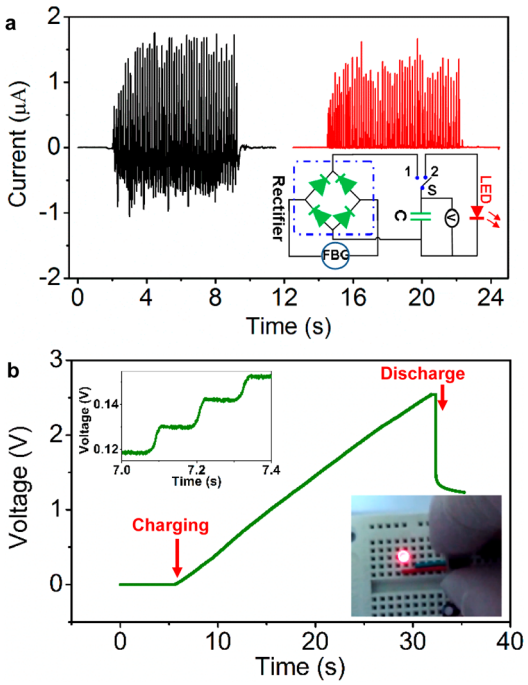

Figure 5. Electricity generation of the "power shirt". (a) Output current of the "power shirt" with (black curve) and without (red curve) rectification when the lab coat was being shaken. The inset depicts the equivalent loop circuit for storing the electrical energy produced by the "power shirt" and lighting the LED. (b) Voltage charging curve of a 2.2 μF commercial capacitor by the "power shirt". The upper inset shows an enlarged plot during charging. The lower inset depicts digital photography of a lighted LED powered by the charged capacitor.

To rule out the possible artifacts, the measurement of the output current was carried out when two FBGs were connected in parallel with an external load of 80 MΩ under the same frequency and deformation control. As shown in Figure S6b, the total output current was enhanced, indicating that the electricity output of the FBGs satisfied a linear superposition criterion in the basic circuit connections.

The stability of the FBG is an essential factor to ensure its practical applications. In our study, the FBG was continuously operated for 90 000 cycles at a stimulation strain of 2.15% and frequency of 5 Hz. Typical data in 1 min for every hour are shown in Figure 3e, and only a small variation of peak output current is seen in Figure 3f, indicating the highly stable power generation of the FBG. This feature may be attributed to the robustness of the device, as no noticeable surface morphology degradation of the PCCT and CCT after the test was proven from the SEM analysis (Figure S7).

Fiber-Based Generator as an Active Sensor for Body Motion Detection. A single FBG was fixed on a subject's index finger. We checked the output current flowing through an external load of 80 MΩ at five different bending–releasing motion states that were labeled as state I, II, III, IV, and V, respectively (insets in Figure 4a). In each motion state, the finger was bent to the same amplitude and then released for three cycles. It can be seen that a couple of output current signals with opposite polarity would be generated in every bending–releasing motion cycle (Figure 4a). The instantaneous output power generated by the FBG with small-scale finger motion could reach ~0.91 μW (average area power density of ~0.1 μW/cm^2, Supplementary Note 1), which was enough to power an electronic device such as a liquid crystalline display (LCD) with small power consumption (Supplementary Video 1 and Figure S8). As discussed above, the peak output currents were decided by both motion speed and motion amplitude. However, in our experiments, the finger motion speed was manually controlled; thus, a small fluctuation is possible (Figure S9a). As the total charge transfer corresponds only to the motion amplitude regardless of the motion speed, we have integrated each positive current peak for five different motion states, as shown in Figure S9b and Figure 4b, indicating that the total amount of charges transferred increased with the increase of motion amplitude, from which the motion states were quantitatively identified. This behavior indicates that the FBG can be used as a self-powered active sensor[28,35–37] for detecting tiny muscle motion/stretching without an external power at least for the sensor unit and has potential applications in patients' rehabilitation training and sports training.

Power Shirt for Health Monitoring. For this demonstration, eight FBGs were woven into a fabric and connected in parallel (Figure 1h), then the fabric was sew on a lab coat to fabricate a "power shirt" (Figure 6b). When the lab coat was shaken, an alternating output current would be generated (black curve in Figure 5a).

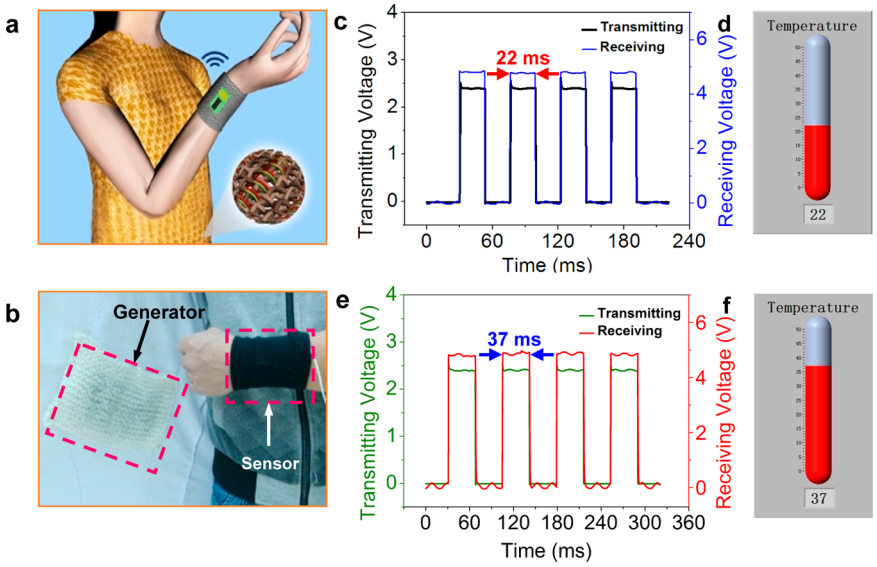

Figure 6. Wireless body temperature sensor system triggered by the "power shirt". (a) Schematic diagram and (b) digital photography of a wireless body temperature monitor system triggered by the power clothes. Modulated and demodulated signals that represent the temperatures detected by the sensor when the wristband was placed (c) on a desk or (e) on a human wrist. The corresponding temperature values of (d) 22 °C for room temperature and (f) 37 °C for body temperature are shown in the display screen.

Additionally, an approach to prove the electricity generated by FBGs has also been implemented. As illustrated in Figure S10, when shaking only the electrodes that were fixed on the lab coat, there were no signals detected by the measuring instrument. The output electric signals were first rectified by a bridge rectifier (inset in Figure 5a), transforming alternating current to direct current (red curve in Figure 5a) and charging the capacitor continuously (Supplementary Videos 2). The charging curve of the 2.2 μF commercial capacitor is shown in Figure 5b. The capacitor could be charged to 2.4 V in around 27 s, and every step of voltage increase corresponded to each vibration of the lab coat (upper-left inset in Figure 5b). After the capacitor was fully charged, it could light up a red light emitting diode (LED), as shown in the lower-right inset of Figure 5b, indicating that the electricity generated by the "power shirt" can be stored in a storage cell and power commercial electronics.

Furthermore, the "power shirt" had successfully triggered a homemade wireless body temperature monitoring system. The working principle of the wireless body temperature monitor system is schematically shown in Figure 6a and Figure S11. The "power shirt" was used to charge a 10 nF capacitor; when the voltage of the capacitor reached a threshold of 2.4 V, it would wake up a microcontroller unit (MCU, Atmega168 V-10PI, with a power consumption of 0.18 μW in standby mode and 27 μW in active mode) that was driven by an external power source. The MCU issued instructions to the thermistor integrated into the wristband to detect surrounding temperature and converted the detected temperature analog signals into digital signals by an analog−digital (AD) module. Then, the digital signals were loaded directly into a square wave generated by the MCU in which the half-period of the wave indicated the temperature value and was transmitted by an infrared diode. Finally, the receiver infrared diode simultaneously captured the signals that were demodulated by another MCU and identified the temperature value, and sent the information to the display screen.

In our study, the active body temperature monitor system detected the surrounding temperature where the wristband was worn when shaking the lab coat (Supplementary Videos 3). The modulated signals shown in Figure 6c and e represent the detected temperatures when the wristband was placed on a desk or on the human wrist, respectively. Meanwhile, the corresponding temperature values of 22 °C for room temperature and 37 °C for body temperature are shown in the display (Figure 6d and f).

CONCLUSIONS

In summary, we have fabricated a flexible and metal-free FBG *via* a cost-effective method by using commodity cotton threads, a PTFE aqueous suspension, and carbon nanotubes as source materials. The FBG can convert biomechanical motions/vibration energy into electricity utilizing the electrostatic effect with an average output power density of ~0.1 μW/cm^2. The FBG was demonstrated as a self-powered active sensor to quantitatively detect human motion. Furthermore, FBGs had been identified as an effective building element for a power shirt that could trigger a wireless homemade body temperature sensor system. This work establishes the first proof-of-concept that FBGs

can be woven into textiles and extract energy from biomechanical motions for powering mobile medical systems, making the self-powered smart garment possible.

EXPERIMENTAL SECTION

Fabrication of CNT Ink. First, CNTs were treated with 5 M nitric acid for 30 min to increase the hydrophilicity. Then 20 mg/mL acid pretreated CNTs and 40 mg/mL sodium dodecyl benzenesulfonate (SDBS) were dispersed in deionized water. Last, the mixture was sonicated for 20 min using an ultrasonic cell disruptor (Kesheng Sonics Vibra Cell, 550 F).

Fabrication of CCT. Since the surface of the commercial cotton threads was fibrous, the cotton threads were first treated with an ethanol flame to eliminate redundant fibers. Then they were cleaned by acetone, ethanol, and deionized water several times, following by immersing into 5 M nitric acid solution for 1 h to increase the hydrophilicity. The cotton threads were coated by CNTs by using the CNT ink mentioned above through the "dipping and drying" method.[38] Specifically, the treated cotton threads were alternately dipped into the CNT ink and dried at 80 °C in an oven. After this process was repeated several times, the conductive cotton threads kept dry at 80 °C in an oven for 2 h.

Fabrication of PTFE and PCCT. The PCCT was fabricated through the "dipping and drying" method as well. Typically, the CCT was immersed into PTFE solution (Aladdin, 60% wt, aqueous) for 30 s and then dried at 60 °C for 5 min. The "dipping and drying" process was repeated three times to ensure that the CCT was completely coated by PTFE. The resulting PCCT was then annealed at 150 °C in an oven for 12 h. Finally, the PCCTs were polarized *via* the plasma method with a service power of 120 W for 40 min.

Assembly of FBG and the "Power Shirt". A CCT and a PCCT were entangled with each other to form a double-helix-structure device. The helix turns and leaving gaps of the FBG can be adjusted, and the two ends of the FBG were fixed by commodity cotton threads. Then the FBGs were woven into the fabric to form a "power shirt".

Characterization. The morphology of the samples was probed by a high-resolution field emission scanning electron microscope (FEI Nova NanoSEM 450). The conductance of the CCT was studied by a Keithley 2400 source meter. The mechanical property of the CCT was characterized by an electronic universal material testing machine (RGM-4005T, Reger, China). The plasma polarization method was carried out with a PDC-MG gas plasma dry cleaner (Hengming, China). The surface potential of PTFE was detected by an electrometer (EST102, Huajing Beijing, China). The periodic stretching−releasing process of the FBG was stimulated by a resonator (JZK, Sinocera, China), which was controlled by a swept signal generator (YE 1311-D, Sinocera, China). The power generation performance measurement system of the FBG is schematically shown in Figure S4, in which one end of the FBG was fixed on an *x-y-z* mechanical stage that was mounted tightly on an optical table, while the other end was fixed on the resonator. During the measurement process, a single FBG was periodically stretched and released with different degrees of strain and frequency by the resonator (JZK). Simultaneously, the current signals through an external load of 80 MΩ were measured by a Stanford low-noise current preamplifier (model SR570). The modulated and demodulated signals generated by the wireless body temperature sensor system were monitored by an Agilent DSOX-2014 oscilloscope.

Conflict of Interest: The authors declare no competing financial interest.

Acknowledgment. This work was financially supported by the National Natural Science Foundation of China (51322210, 51002056), a Foundation for the Author of National Excellent Doctoral Dissertation of PR China (201035), the Fundamental Research Funds for the Central Universities (HUST: 2012YQ025, 2013YQ049, 2013TS160), and the seed project of Wuhan National Laboratory for Optoelectronics. The authors would like to thank Prof. J. Tang and Dr. F. R. Fan for their constructive suggestions.

Supporting Information Available: More detailed information about calculations, sensor working principle, *I*−*V* curve of CCT, surface potential of PTFE, supporting movies 1−3, *etc.* This material is available free of charge *via* the Internet at http://pubs.acs.org.

REFERENCES AND NOTES

1. Rogers, J. A. Electronics: A Diverse Printed Future. *Nature* **2010**, *468*, 177–178.
2. Yamada, T.; Hayamizu, Y.; Yamamoto, Y.; Izadi-Najafabadi, A.; Futaba, D. N.; Hata, K. A Stretchable Carbon Nanotube Strain Sensor for Human-Motion Detection. *Nat. Nanotechnol.* **2011**, *6*, 296–301.
3. Wang, C.; Hwang, D.; Yu, Z.; Takei, K.; Park, J.; Chen, T.; Ma, B.; Javey, A. User-Interactive Electronic Skin for Instantaneous Pressure Visualization. *Nat. Mater.* **2013**, *12*, 899–904.
4. Lipomi, D. J.; Vosgueritchian, M.; Tee, B.; Hellstrom, S. L.; Lee, J. A.; Fox, C. H.; Bao, Z. Skin-Like Sensors of Pressure and Strain Enabled by Transparent, Elastic Films of Carbon Nanotubes. *Nat. Nanotechnol.* **2011**, *6*, 788–792.
5. Ross, P. Managing Care through the Air. *IEEE Spectrum* **2004**, *6*, 26–31.
6. Flowerday, A.; Smith, R. Lessons Learnt from Long-Term Chronic Condition Monitoring. *Proc. 1st Int. Workshop Wearable Implantable Body Sensor Network* **2004**, 48.
7. Needham, P.; Gamlyn, L. Arrhythmia Analysis in the Community. *Proc. 1st Int. Workshop Wearable Implantable Body Sensor Network* **2004**, 49–50.
8. Wolffenbuttel, M. R.; Regtien, P. P. L. Polysilicon Bridges for the Tealization of Tactile Sensors. *Sens. Actuators, A* **1991**, *26*, 257–264.
9. Chu, Z.; Sarrob, P. M.; Middelhoeka, S. Silicon Three-Axial Tactile Sensor. *Sens. Actuators, A* **1996**, *54*, 505–510.
10. Jost, K.; Stenger, D.; Perez, C. R.; McDonough, J. K.; Lian, K.; Gohotsi, Y.; Dion, G. Knitted and Screen Prited Carbon-Fiber Supercapacitors for Applications in Wearable Electronics. *Energy Environ. Sci.* **2013**, *6*, 2698–2705.
11. Hu, L.; Pasta, M.; Mantia, F. L.; Cui, L.; Jeong, S.; Deshazer, H. D.; Choi, J.; Han, S.; Cui, Y. Porous, and Conductive Energy Textiles. *Nano Lett.* **2010**, *10*, 708–714.
12. Lee, Y.; Kim, J.; Lee, J.; Kim, H.; Choi, S.; Seo, J.; Jeon, S.; Kim, T.; Lee, J.; Choi, J. Wearable Textile Battery Rechargeable by Solar Energy. *Nano Lett.* **2013**, *13*, 5753–5761.
13. Chen, T.; Qiu, L.; Yang, Z.; Cai, Z.; Ren, J.; Li, H.; Lin, H.; Sun, X.; Peng, H. An Integrated Energy Wire for Both Photoelectric Conversion and Storage. *Angew. Chem., Int. Ed.* **2012**, *51*, 11977–11980.
14. Qi, Y.; McAlpine, M. C. Nanotechnology-Enabled Flexible and Biocompatible Energy Harvesting. *Energy Environ. Sci.* **2010**, *3*, 1275–1285.
15. Starner, T. Human-Powered Wearable Computing. *IBM Syst. J.* **1996**, *35*, 618–629.
16. Rome, L. C.; Flynn, L.; Goldman, E. M.; Yoo, T. D. Generating Electricity While Walking with Loads. *Science* **2005**, *309*, 1725–1728.
17. Donelan, J. M.; Li, Q.; Naing, V.; Hoffer, J. A.; Weber, D. J.; Kuo, A. D. Biomechanical Energy Harvesting: Generating Electricity during Walking with Minimal User Effort. *Science* **2008**, *319*, 807–810.
18. Nelson, L.; Bowen, C.; Stevens, R.; Cain, M.; Stewart, M. Modelling and Measurement of Piezoelectric Fibers and Interdigitated Electrodes for the Optimisation of Piezofiber Composites. *SPIE Conf. Proc.* **2003**, *5053*, 556–567.
19. Wang, Z. L.; Song, J. Piezoelectric Nanogenerators Based on Zinc Oxide Nanowire Arrays. *Science* **2006**, *312*, 242–246.

20. Qin, Y.; Wang, X.; Wang, Z. L. Microfibre-Nanowire Hybrid Structure for Energy Scavenging. *Nature* **2008**, *451*, 809–813.
21. Qin, Y.; Jafferis, N. T.; Lyons, K.; Christine, J.; Lee, M.; Ahmad, H.; McAlpine, M. C. Piezoelectric Ribbons Printed onto Rubber for Flexible Energy Conversion. *Nano Lett.* **2010**, *10*, 524–528.
22. Park, K.; Lee, M.; Liu, Y.; Moon, S.; Hwang, G.; Zhu, G.; Kim, J.; Kim, S.; Kim, D.; Wang, Z. L.; *et al*. Flexible Nanocomposite Generator Made of $BaTiO_3$ Nanoparticles and Graphitic Carbons. *Adv. Mater.* **2012**, *24*, 2999–3004.
23. Lee, K.; Kumar, B.; Seo, J.; Kim, K.; Sohn, J.; Cha, S.; Choi, D.; Wang, Z. L.; Kim, S. P-Type Polymer-Hybridized High-Performance Piezoelectric Nanogenerators. *Nano Lett.* **2012**, *12*, 1959–1964.
24. Chang, C.; Tran, V. H.; Wang, J.; Fuh, Y. K.; Lin, L. Direct-Write Piezoelectric Polymeric Nanogenerator with High Energy Conversion Efficiency. *Nano Lett.* **2010**, *10*, 726–731.
25. Persano, L.; Dagdeviren, C.; Su, Y.; Zhang, Y.; Girarod, S.; Pisignano, D.; Huang, Y.; Rogers, J. A. High Performance Piezoelectric Devices Based on Aligned Arrays of Nanofibers of Poly(vinylidenefluoride-*co*-trifluoroethylene). *Nat. Commun.* **2012**, *4*, 1633.
26. Lee, B.; Zhang, J.; Zueger, C.; Chung, W.; Yoo, S. Y.; Wang, E.; Meyer, J.; Ramesh, R.; Lee, S. Virus-Based Piezoelectric Energy Generation. *Nat. Nanotechnol.* **2012**, *7*, 351–356.
27. Sun, C.; Shi, J.; Bayerl, D. J.; Wang, X. PVDF Microbelts for Harvesting Energy from Respiration. *Energy Environ. Sci.* **2011**, *4*, 4508–4512.
28. Zhong, Q. Z.; Zhong, J. W.; Hu, B.; Hu, Q.; Zhou, J.; Wang, Z. L. Paper-Based Nanogenerator As Power Source and Active Sensor. *Energy Environ. Sci.* **2013**, *6*, 1779–1784.
29. Boland, J.; Chao, Y.; Suzuki, Y.; Tai, Y. C. Micro Electret Power Generator. *Proc. 16th IEEE Int. Conf. MEMS* **2003**, 538–541.
30. Fan, F.; Tian, Z.; Wang, Z. L. Flexible Triboelectric Generator. *Nano Energy* **2012**, *1*, 328–334.
31. Zhang, X.; Han, M.; Wang, R.; Zhu, F.; Li, Z.; Wang, W.; Zhang, H. Frequency-Multiplication High-Output Triboelectric Nanogenerator for Sustainably Powering Biomedical Microsystems. *Nano Lett.* **2013**, *13*, 1168–1172.
32. Post, E. R.; Waal, K. Electrostatic Power Harvesting in Textiles. *Proc. ESA Ann. Meet. Electrost.* **2010**, Paper G1.
33. Hu, L.; Choi, J.; Yang, Y.; Jeong, S.; Mantia, F. L.; Cui, L.; Cui, Y. P. Highly Conductive Paper for Energy-Storage Devices. *Natl. Acad. Sci. U.S.A.* **2009**, *106*, 21490–21494.
34. Malecki, J. A. Linear Decay of Charge in Electrets. *Phys. Rev. B* **1999**, *59*, 9954–9960.
35. Lee, S.; Hinchet, R.; Lee, Y.; Yang, Y.; Lin, Z.; Ardila, G.; Montes, L.; Mouis, M.; Wang, Z. L. Ultrathin Nanogenerators as Self-Powered/Active Skin Sensors for Tracking Eye Ball Motion. *Adv. Funct. Mater.* **2013**, *24*, 1163–1168.
36. Hu, Y.; Yang, J.; Jing, Q.; Niu, S.; Wu, W.; Wang, Z. L. Triboelectric Nanogenerator Built on Suspended 3D Spiral Structure as Vibration and Positioning Sensor and Wave Energy Harvester. *ACS Nano* **2013**, *7*, 10424–10432.
37. Lin, L.; Xie, Y.; Wang, S.; Wu, W.; Niu, S.; Wen, X.; Wang, Z. L. Triboelectric Active Sensor Array for Self-Powered Static and Dynamic Pressure Detection and Tactile Imaging. *ACS Nano* **2013**, *7*, 8266–8274.
38. Liu, N. S.; Ma, W. Z.; Tao, J. Y.; Zhang, X. H.; Su, J.; Li, L. Y.; Yang, C. X.; Gao, Y. H.; Golberg, D.; Bando, Y. Cable-Type Supercapacitors of Three-Dimensional Cotton Thread Based Multi-Grade Nanostructures for Wearable Energy Storage. *Adv. Mater.* **2013**, *25*, 4925–4931.